

ComMark: Covert and Robust Black-Box Model Watermarking with Compressed Samples

Yunfei Yang^{1,2,3}, Xiaojun Chen^{1,2,3*}, Zhendong Zhao^{1,2}, Yu Zhou⁴, Xiaoyan Gu^{1,2,3}, Juan Cao⁵

¹Institute of Information Engineering, Chinese Academy of Sciences, Beijing, China

²State Key Laboratory of Cyberspace Security Defense, Beijing, China

³School of Cyber Security, University of Chinese Academy of Sciences, Beijing, China

⁴College of Computer Science, Nankai University, Tianjin, China

⁵Institute of Computing Technology, Chinese Academy of Sciences, Beijing, China

{yangyunfei, chenxiaojun, zhaozhendong, guxiaoyan}@iie.ac.cn

yzhou@nankai.edu.cn, caojuan@ict.ac.cn

Abstract

The rapid advancement of deep learning has turned models into highly valuable assets due to their reliance on massive data and costly training processes. However, these models are increasingly vulnerable to leakage and theft, highlighting the critical need for robust intellectual property protection. Model watermarking has emerged as an effective solution, with black-box watermarking gaining significant attention for its practicality and flexibility. Nonetheless, existing black-box methods often fail to better balance covertness (hiding the watermark to prevent detection and forgery) and robustness (ensuring the watermark resists removal)—two essential properties for real-world copyright verification. In this paper, we propose ComMark, a novel black-box model watermarking framework that leverages frequency-domain transformations to generate compressed, covert, and attack-resistant watermark samples by filtering out high-frequency information. To further enhance watermark robustness, our method incorporates simulated attack scenarios and a similarity loss during training. Comprehensive evaluations across diverse datasets and architectures demonstrate that ComMark achieves state-of-the-art performance in both covertness and robustness. Furthermore, we extend its applicability beyond image recognition to tasks including speech recognition, sentiment analysis, image generation, image captioning, and video recognition, underscoring its versatility and broad applicability.

1. Introduction

Deep neural networks [5, 55, 59] have been widely applied in fields such as face recognition [33], autonomous driving



Figure 1. Examples of watermark samples from existing black-box methods including Abstract [1], Content [76], EWE [28], MEAD [42] and BlindMark [35].

[18], and content generation [15]. Building state-of-the-art models demands significant investment in large-scale data collection and annotation, algorithm design, and computational resources. These models embody valuable intellectual property but are vulnerable to unauthorized reproduction, dissemination, and derivation [60], highlighting the urgent need for effective protection.

Model watermarking [11, 47, 65, 77, 78], which embeds hidden information into model parameters or outputs, has emerged as a promising solution. Techniques are generally classified into white-box and black-box schemes. White-box methods [41, 66, 72] require full access to model internals during verification, which is often impractical in real-world settings. In contrast, black-box watermarking [28, 60, 82] only requires querying the model with crafted samples and inferring ownership from predictions, making it more practical and widely adopted.

Despite their potential, existing black-box methods struggle to balance covertness and robustness. Some [28, 42, 76] offer strong robustness against removal attacks but lack visual stealth, making watermark samples easily detectable or forgeable. Others [29, 35, 70] achieve higher covertness, with samples nearly indistinguishable from clean data, but sacrifice robustness. Designing black-box watermarks that ensure both remains an open challenge.

We identify a key limitation: most prior methods con-

*Corresponding author.

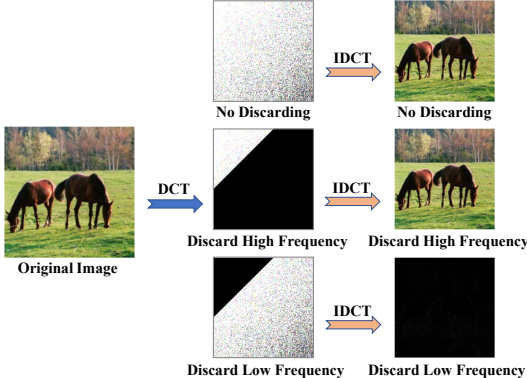


Figure 2. The effect of visual differences in the spatial domain resulting from different components being discarded in the frequency domain. The DCT and IDCT are the discrete cosine transform and its inverse transform, respectively.

struct watermarks in the spatial domain at pixel level, often embedding features in only part of the sample (see Figure 1). These designs are both fragile and conspicuous, rendering them vulnerable to cropping, scaling [69], JPEG compression [46], model extraction [49], and forgery [34], potentially leading to verification failures. To address this, we propose embedding covert watermark signals across the entire sample.

Frequency-domain transformations [26, 30, 38, 74, 81] decompose spatial features into frequencies, enabling global processing (Figure 2). Leveraging this, we first transform training samples into the frequency domain. Inspired by lossy image compression [9, 10, 14, 19, 21, 73], we avoid embedding explicit signals to prevent reverse inspection. Instead, we discard high-frequency components via quantization—imperceptible to human vision—and reconstruct the samples. These globally removed components create watermark samples whose trigger condition is compression behavior rather than pixel-level patterns, enabling both high covertness and robustness. To further enhance robustness and prevent false triggering, we simulate common input preprocessing attacks for joint training and introduce a similarity loss to cluster watermark samples with the same label in feature space, reinforcing their link to the watermark target label. Our main contributions are:

- **Novel Approach for Watermark Sample Construction.** We introduce a new approach to constructing watermark samples in frequency domain, using global compression behavior as watermark triggering signal. Compared to prior methods, this is more covert, and its global distribution property enhances the watermark robustness.
- **Covert and Robust Watermarking Framework.** We propose ComMark, a black-box watermarking framework that balances better covertness and robustness. Our framework includes frequency-domain compression for constructing watermark samples, attack simulation strat-

egy to boost robustness and prevent false triggering, and similarity loss to improve feature-level robustness. Our source code is available at [8].

- **Comprehensive Performance Evaluation.** We compare ComMark with state-of-the-art black-box watermarking techniques on multiple datasets. Our results demonstrate its superior performance across effectiveness, covertness, and robustness. Additionally, we test various watermark triggering conditions, confirming no false triggering. Extending our approach to audio, video, and text modalities yields consistently strong performance, showcasing its generalizability.

2. Related Work

Black-box watermarking methods [17, 40, 45] verify ownership without accessing model parameters, relying on whether watermark samples elicit target predictions. The earliest approach, Abstract [1], was inspired by backdoor learning and used out-of-distribution (OOD) images as triggers. Content [76] embedded patterns (e.g., text) into clean samples and linked them to target labels. MEAD [42] generated composite samples by combining two task categories, enhancing watermark persistence in stolen models. While these methods offer robustness, their watermarks are often visually obvious, enabling adversaries to bypass verification. To improve covertness, BlindMark [35] used an encoder-discriminator framework to embed fixed OOD images into clean data. MAB [29] assigned random labels to clean samples and applied projected gradient ascent to push them away from decision boundaries, creating imperceptible watermarks. However, such methods often lack robustness.

In contrast, we propose a novel watermarking technique inspired by JPEG compression [4, 6, 16, 21, 64]. By quantizing frequency-domain features to remove high-frequency components, we generate global, hard-to-remove triggers. These modifications remain imperceptible in the spatial domain, achieving both strong covertness and robustness.

3. Proposed Method

3.1. Threat Model

Adversary: After obtaining the victim model via replication or extraction, the adversary attempts to invalidate watermark verification. This may involve removal attacks (e.g., finetuning, pruning) or preprocessing the defender’s verification samples through cropping, scaling, rotation, or JPEG compression to hinder ownership verification. Another potential threat is that the adversary could embed their own forged watermark into the model or discover samples that cause false triggering, potentially leading to disputes over ownership.

Defender: The defender, as the model owner, controls

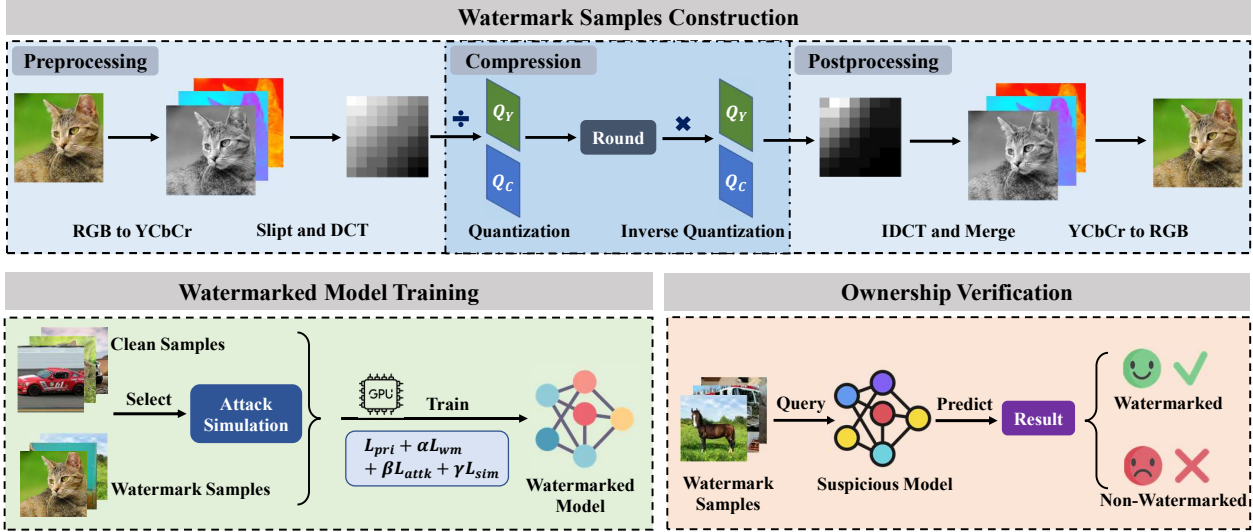


Figure 3. An overview of our ComMark method.

the training process and embeds the watermark before deployment. Given unknown future attacks, the goal is to craft a watermark that is effective, imperceptible, and robust. Verification is conducted in a black-box setting, where the defender only accesses the model’s predictions via an API controlled by the adversary.

3.2. Overview

Our method, illustrated in Figure 3, proceeds as follows: the defender selects a subset of clean samples and compresses them via Watermark Samples Construction module, assigning them a predefined target label to form the watermark set. During Watermarked Model Training, the model is trained on both clean and watermark data, with a portion of data undergoing adversarial processing each epoch. Finally, in Ownership Verification, defender queries the suspicious model with watermark test samples and, if the target class prediction rate exceeds a threshold, attributes the ownership.

3.3. Watermark Samples Construction

Previous watermarking methods typically constructed watermark samples in the spatial domain, where watermark triggers relied on fixed pixel-level feature patterns (often localized in specific regions). This reliance made such watermarking methods susceptible to detection or removal. To address these issues, inspired by JPEG compression algorithm, we propose constructing watermark samples in the frequency domain, leveraging quantization-based compression behavior as the triggering pattern. This novel black-box watermarking approach ensures superior covertness and robustness. Our construction process involves three stages: preprocessing, compression, and postprocessing.

Preprocessing. We first convert input images from RGB to

YCbCr, separating luminance (Y) from chrominance (Cb, Cr) components, as human vision is more sensitive to luminance. This separation allows selective compression.

Images are resized to $H \times H$ (with H divisible by 8) and split into 8×8 blocks. Each block undergoes a 2D Discrete Cosine Transform (DCT) [2], converting it into frequency domain:

$$F(u, v) = \alpha(u)\alpha(v) \sum_{i=0}^{N-1} \sum_{j=0}^{N-1} f(i, j) \cos\left[\frac{(2i+1)u\pi}{2N}\right] \cos\left[\frac{(2j+1)v\pi}{2N}\right]$$

$$\alpha(u) = \begin{cases} \sqrt{1/N}, & u = 0 \\ \sqrt{2/N}, & u \neq 0 \end{cases} \quad \alpha(v) = \begin{cases} \sqrt{1/N}, & v = 0 \\ \sqrt{2/N}, & v \neq 0 \end{cases} \quad (1)$$

where $F(u, v)$ represents the intensity at position (u, v) in frequency domain, and $f(i, j)$ represents the pixel value at position (i, j) in spatial domain. DCT is used over DFT due to its superior energy compaction, making it well-suited for compression.

Compression. In the frequency domain, we apply quantization to suppress high-frequency components, which correspond to fine details less visible to the human eye. Low-frequency components—carrying primary visual content—are largely retained. Different quantization tables are used for Y and Cb/Cr channels to reflect human visual sensitivity. This results in globally distributed, covert watermark signals. The quantization and inverse quantization processes are expressed as:

$$F_q(u, v) = \begin{cases} \text{Round}\left[\frac{F(u, v)_Y}{Q_Y(u, v)}\right] \times Q_Y(u, v) \\ \text{Round}\left[\frac{F(u, v)_{CbCr}}{Q_C(u, v)}\right] \times Q_C(u, v) \end{cases} \quad (2)$$

where $\text{Round}(\cdot)$ is the rounding operation. Q_Y and Q_C are the quantization tables for luminance and chrominance components, respectively. They are adapted based on the

compression quality factor using the standard JPEG quantization table Q_S [31], calculated as:

$$Q(i, j) = \begin{cases} \frac{50 \times Q_S(i, j)}{Factor}, & Factor \leq 50 \\ \frac{(200 - 2 \times Factor) \times Q_S(i, j)}{100}, & Factor > 50 \end{cases} \quad (3)$$

where Q represents Q_Y or Q_C , and $Factor$ is the quality factor ranging from 0 to 100.

Postprocessing. After quantization-based compression, we first perform inverse DCT (IDCT) on each block to return to spatial domain:

$$f_q(i, j) = \alpha(u)\alpha(v) \sum_{u=0}^{N-1} \sum_{v=0}^{N-1} F_q(u, v) \cos\left[\frac{(2i+1)u\pi}{2N}\right] \cos\left[\frac{(2j+1)v\pi}{2N}\right] \quad (4)$$

where the symbols retain the same meanings as in DCT.

Next, we reassemble the blocks into a full $H \times H$ image, and convert the image back to RGB space.

Following above procedures, we can generate a sufficient number of watermark training and verification samples for subsequent use.

3.4. Watermarked Model Training

Composition of Training Dataset. We randomly sample part of the original training data, relabel it to a predefined randomly selected watermark target label y_t^w , and form the watermark dataset D_w . The rest constitutes the primary task dataset D_p . To enhance robustness and reduce the risk of false activation from benign augmentations, we simulate attacks during training. Specifically, in each epoch, we first randomly select a portion p from both D_p and D_w , obtaining D'_p and D'_w :

$$D'_p = \text{Sample}_{rand}(D_p, p|D_p|), \quad D'_w = \text{Sample}_{rand}(D_w, p|D_w|) \quad (5)$$

where $\text{Sample}_{rand}(D, n)$ represents randomly sampling n samples from dataset D without replacement.

Each replicated dataset is then partitioned into k non-overlapping subsets. The i -th subset is subjected to attack A_i as follows:

$$\begin{aligned} D_p^{A_i} &= \text{ApplyAttack}(A_i, \text{Split}(D'_p, i, k)) \\ D_w^{A_i} &= \text{ApplyAttack}(A_i, \text{Split}(D'_w, i, k)) \end{aligned} \quad (6)$$

where $\text{Split}(D, i, k) = \{x_j \in D | j \equiv i \pmod k\}$ denotes partitioning D into k subsets and returning the i -th subset. $\text{ApplyAttack}(A, D)$ applies attack A to dataset D , returning the attacked version. In this work, we utilize 10 common data preprocessing attacks (i.e., $k=10$), including cropping, rotation, scaling, Gaussian noise, Gaussian blur, brightness change, image quantization, JPEG2000 compression, WEBP compression, and color quantization. For each epoch, all the attacked data together form the attacked dataset D_a .

Table 1. Comparison of effectiveness and harmlessness (%).

Method	GTSRB		CIFAR10		CIFAR100		VGGFace	
	Acc↑	WSR↑	Acc↑	WSR↑	Acc↑	WSR↑	Acc↑	WSR↑
Clean Model	95.59	2.32	89.79	9.48	66.09	1.03	52.37	0.96
Abstract	93.23	100.00	88.53	100.00	65.19	100.00	51.93	100.00
Content	93.50	99.29	88.22	99.96	63.41	99.93	49.99	99.99
MEAD	94.03	99.72	88.89	100.00	65.04	100.00	51.66	98.00
Noise	92.18	99.76	87.73	99.92	64.58	99.50	50.38	99.91
BlindMark	92.30	94.80	87.70	99.80	64.51	97.80	51.59	99.80
MAB	93.74	100.00	87.84	100.00	64.39	100.00	51.75	100.00
ComMark	94.06	99.83	88.12	100.00	65.06	100.00	51.79	99.71

Design of Training Loss. We first apply the regular classification loss on the three training sub-datasets, i.e.,

$$\begin{aligned} L_{pri} &= \sum_{x_i^p \in D_p} \mathcal{L}(f_\theta(x_i^p), y_i^p) \\ L_{wm} &= \sum_{x_i^w \in D_w} \mathcal{L}(f_\theta(x_i^w), y_t^w) \\ L_{attk} &= \sum_{x_i^a \in D_a} \mathcal{L}(f_\theta(x_i^a), y_i^a) \end{aligned} \quad (7)$$

where f_θ is a model parameterized by θ and \mathcal{L} is cross-entropy loss.

To further improve the correlation between watermark samples and the target label, we introduce a similarity loss L_{sim} that pulls same-label samples closer and pushes different-label samples apart. We adopt contrastive loss [23] to achieve this:

$$L_{sim} = \frac{1}{2N} \sum_{i=1}^N [y_i \cdot d_i^2 + (1-y_i) \cdot \max(\text{margin} - d_i, 0)^2] \quad (8)$$

where d_i is the Euclidean distance of the i -th sample pair, and $y_i = 1$ if the labels match, 0 otherwise. The margin defines the minimum distance between sample features of different labels.

Thus, the total training loss for watermarked model is:

$$L = L_{pri} + \alpha L_{wm} + \beta L_{attk} + \gamma L_{sim} \quad (9)$$

where α , β , and γ are coefficients that balance these losses.

3.5. Ownership Verification

To verify ownership, the defender queries the suspicious model with watermark test samples in D_v , all labeled with the target class. The watermark success rate Acc_{wm} is then computed. If Acc_{wm} exceeds a predefined threshold, ownership is confirmed. A higher Acc_{wm} indicates stronger ownership evidence under black-box scenarios.

4. Experiments

4.1. Experimental Setup

Tasks, Datasets, and Models. We evaluate ComMark on three tasks across four datasets: traffic sign recognition (GTSRB [58]), object classification (CIFAR10, CIFAR100

Table 2. Comparison of robustness (%) against soft and hard label settings for three popular model extraction attacks. These results are obtained through testing on stolen models. The performance of victim model is presented in Table 1.

Dataset	Method	Distillation				JBDA				Knockoff			
		Soft Label		Hard Label		Soft Label		Hard Label		Soft Label		Hard Label	
		Acc	WSR \uparrow	Acc	WSR \uparrow	Acc	WSR \uparrow	Acc	WSR \uparrow	Acc	WSR \uparrow	Acc	WSR \uparrow
GTSRB	Abstract	65.50	28.00	86.17	9.00	88.88	31.00	75.01	6.00	79.45	100.00	67.56	88.00
	Content	50.71	94.80	47.05	87.34	76.43	99.81	65.44	88.31	81.72	99.99	18.15	99.96
	MEAD	78.73	4.03	64.83	0.28	83.17	26.53	72.75	3.47	89.69	98.06	67.43	85.00
	Noise	3.75	93.77	3.74	92.32	3.73	98.71	4.13	96.33	4.54	99.94	3.56	100.00
	BlindMark	56.83	6.40	53.82	4.60	72.61	10.60	67.62	6.80	76.63	18.40	48.89	9.60
	MAB	60.38	50.51	55.34	46.43	84.70	76.79	83.55	68.11	78.59	82.40	63.99	64.80
	ComMark	25.33	98.99	30.10	98.54	28.31	99.09	20.09	98.73	4.69	100.00	3.74	100.00
CIFAR10	Abstract	52.08	57.00	39.68	11.00	41.93	37.00	47.05	19.00	43.31	74.00	30.58	40.00
	Content	68.85	15.36	40.55	19.06	34.55	12.65	50.14	20.77	53.13	21.09	39.71	15.12
	MEAD	13.59	94.08	20.58	57.90	36.70	92.85	24.10	79.90	35.74	96.88	16.72	89.75
	Noise	49.50	8.37	30.00	19.60	58.71	12.03	40.12	23.92	57.67	15.47	30.26	42.77
	BlindMark	26.95	11.20	41.79	14.20	49.31	14.60	40.02	14.40	32.33	18.20	33.53	12.80
	MAB	59.51	13.40	37.05	12.20	42.99	13.20	38.16	13.60	46.79	12.60	29.04	11.40
	ComMark	62.66	94.51	45.71	84.62	48.88	96.21	40.30	93.03	72.32	98.93	53.80	94.45
CIFAR100	Abstract	20.71	60.00	1.00	10.00	12.99	37.00	12.68	24.00	22.54	84.00	15.44	55.00
	Content	18.00	0.05	2.59	0.04	11.75	0.00	15.44	0.18	18.99	96.22	16.74	54.49
	MEAD	13.26	86.12	1.80	69.00	14.78	91.00	9.93	73.92	20.57	99.27	10.79	93.08
	Noise	13.93	0.00	1.00	0.00	14.69	0.01	12.33	0.33	16.17	0.02	10.08	0.02
	BlindMark	13.02	3.40	5.45	2.20	16.11	2.00	8.73	1.00	29.32	26.40	15.94	4.20
	MAB	18.07	1.80	2.41	0.60	20.29	2.60	12.26	3.80	15.18	2.20	10.20	1.60
	ComMark	22.91	91.61	0.98	75.88	24.67	92.16	18.09	80.30	48.15	99.61	30.84	98.64
VGGFace	Abstract	7.46	21.00	3.63	9.00	12.43	15.00	4.92	12.00	9.48	95.00	2.77	71.00
	Content	8.09	99.84	1.80	87.28	10.21	96.99	4.25	72.04	10.85	99.19	2.38	98.98
	MEAD	8.18	3.00	3.25	4.00	10.00	1.00	6.50	2.00	10.42	87.00	3.73	52.00
	Noise	1.04	89.98	1.00	69.18	1.01	95.49	1.00	78.90	2.85	99.07	1.00	99.12
	BlindMark	10.13	5.20	2.39	0.20	6.85	3.60	5.68	3.40	3.21	30.60	3.22	29.20
	MAB	10.64	27.54	4.28	8.56	7.17	19.25	4.57	16.84	10.02	24.87	3.45	7.75
	ComMark	12.75	96.20	1.09	80.24	6.50	98.94	13.66	81.87	15.63	99.83	3.61	99.84

[32]), and face recognition (VGGFace [51]). ResNet18 [24] is used for GTSRB and CIFAR10, and ResNet34 for CIFAR100 and VGGFace.

Watermark Methods for Comparison. These methods include Abstract [1], Content [76], Noise [76], MEAD [42], BlindMark [35], and MAB [29]. Their detailed introductions are as follows:

- Abstract [1]: Uses abstract art images as watermark samples.
- Content [76]: Adds meaningful text (e.g., "TEST") to normal samples to form watermark samples.
- Noise [76]: Adds Gaussian noise with a specific distribution to normal samples to construct watermark samples.
- MEAD [42]: Selects two categories of normal samples from primary task and then concatenates them to form watermark samples.
- BlindMark [35]: Encodes meaningful images (e.g., copyright logos) into normal images as watermark samples.
- MAB [29]: Randomly selects normal images and changes their labels to random labels as watermark samples, with training using projected gradient ascent to increase the distance between these samples and the decision boundary.

Evaluation Metrics. Effectiveness and robustness are mea-

sured by: (1) Accuracy (Acc): the classification accuracy on primary test sets; (2) Watermark Success Rate (WSR): the percentage of watermark samples classified as the target label.

To assess covertness, we use PSNR [27], SSIM [67], and LPIPS [79] to quantify similarity between watermark and clean images.

Implementation Details. Watermark samples comprise 10% of training data, with a compression quality factor of 90. We train for 100 epochs using Adam (initial learning rate 0.001, decayed by 0.1 every 30 epochs), and set loss weights to $\alpha = 1.0$, $\beta = 1.0$, $\gamma = 0.1$. $margin$ is 1.0 in L_{sim} . Each epoch includes 50% adversarially processed samples. Competing methods and attacks are tuned based on original papers for fair comparison. To eliminate the error influence of randomness, the results reported in our evaluation are the average of five repeated experiments with different random seeds.

4.2. Effectiveness and Harmlessness

In this section, we evaluate the effectiveness and harmlessness of various methods. Table 1 shows our method achieves WSR comparable to SOTA methods on protected

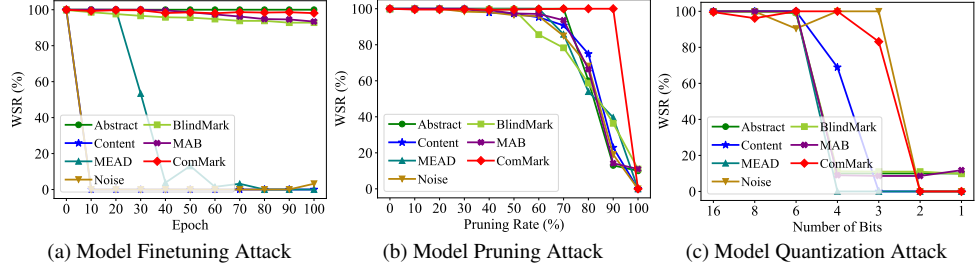


Figure 4. Comparison of robustness against watermark removal attacks. (On CIFAR10)

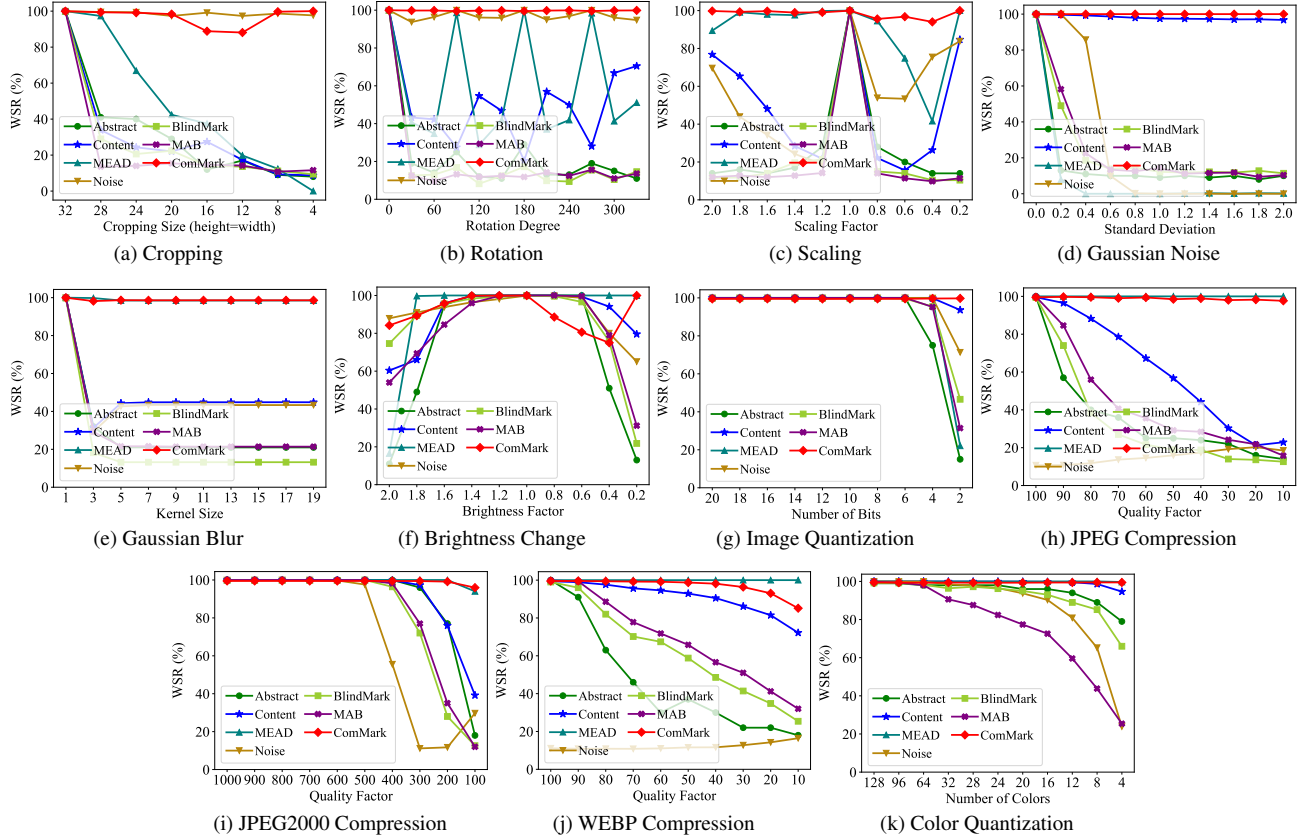


Figure 5. Comparison of robustness against watermark evasion attacks. (On CIFAR10)

model, with rates of 99.83%, 100.00%, 100.00%, and 99.71% on GTSRB, CIFAR10, CIFAR100, and VGGFace datasets, respectively. The primary task accuracy drops by only 1.53%, 1.67%, 1.03%, and 0.58% on these datasets, confirming minimal harm to benign users. While prior methods also achieve similar effectiveness and harmlessness, we highlight that better robustness and covertness of black-box watermarks remain critical challenges.

4.3. Robustness against Extraction Attacks

Model extraction is known to be highly effective in removing watermarks [28, 42, 60, 61], since extracted models often fail to capture watermark triggers that are not tied to the main task. We evaluate ComMark against popular extrac-

tion attacks: Distillation [25], JBDA [50], Knockoff [48], and their hard-label variants. As shown in Table 2, ComMark consistently achieves top watermark success rates, with few exceptions.

Unlike most methods that only perform well in specific settings, ComMark and MEAD show consistent robustness across attacks and datasets. ComMark’s resilience stems from embedding global, covert triggers through JPEG-inspired compression and enforcing feature-space alignment via similarity loss. Further evaluations under Cross-Dataset, Cross-Architecture, and combined attacks (Tables 5-7 of Appendix) confirm ComMark’s superior performance.

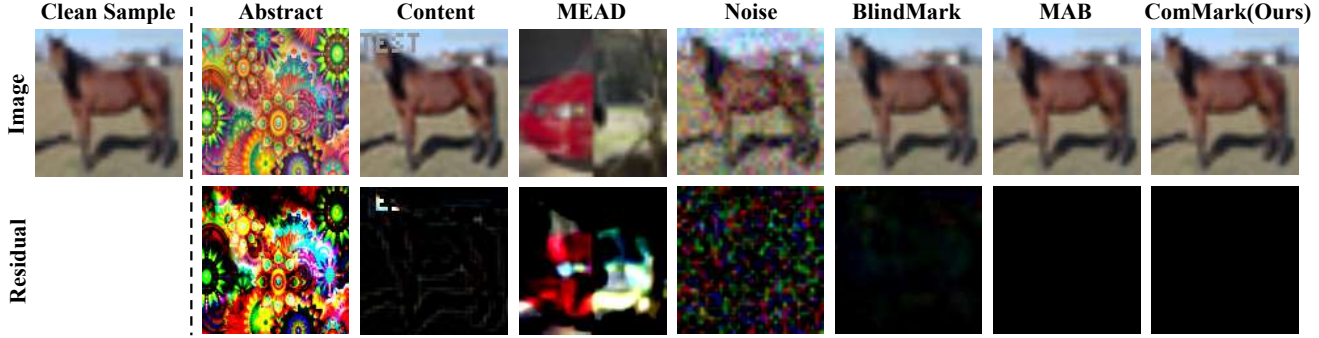


Figure 6. Visual comparison of covertness of different watermarking methods. (On CIFAR10)

Table 3. Quantitative comparison of covertness.

Method	GTSRB			CIFAR10			CIFAR100			VGGFace		
	PSNR \uparrow	SSIM \uparrow	LPIPS \downarrow	PSNR \uparrow	SSIM \uparrow	LPIPS \downarrow	PSNR \uparrow	SSIM \uparrow	LPIPS \downarrow	PSNR \uparrow	SSIM \uparrow	LPIPS \downarrow
Abstract	9.93	0.0733	0.7087	10.92	0.0224	0.6141	10.77	0.0635	0.7107	10.29	0.0330	0.7421
Content	22.37	0.9699	0.0769	26.48	0.9898	0.0421	23.42	0.9859	0.0580	25.46	0.9842	0.0289
MEAD	8.21	0.1322	0.2297	8.65	0.0735	0.6171	10.02	0.0435	0.6573	9.29	0.1371	0.5426
Noise	20.39	0.3741	0.4478	23.70	0.6104	0.4396	23.93	0.5934	0.4049	20.44	0.3647	0.3842
BlindMark	31.24	0.9904	0.0091	36.68	0.9963	0.0079	23.86	0.9407	0.1285	33.22	0.9888	0.0115
MAB	inf	1.0000	0.0000									
ComMark	43.19	0.9976	0.0006	42.85	0.9984	0.0009	42.76	0.9963	0.0010	43.04	0.9986	0.0007

4.4. Robustness against Removal Attacks

We test robustness against three classic removal attacks on CIFAR10. As shown in Figure 4a, ComMark maintains a 98.10% WSR under finetuning, outperforming prior methods, many of which fail significantly. Under 90% pruning (Figure 4b), our WSR remains above 95%, while others drop below 50%. For quantization (Figure 4c), ComMark survives until 2-bit precision, while most competitors fail at 3 or 4 bits. These results highlight the advantage of frequency-domain watermarking over pixel-level methods. Full results on other datasets are in our Appendix B.

4.5. Robustness against Evasion Attacks

To bypass ownership verification, an adversary can use data preprocessing techniques to alter the query samples submitted by defender. We test the robustness of various watermarking methods against 11 input preprocessing attacks [39] on CIFAR10, as shown in Figure 5. Our method outperforms others, maintaining high watermark success rates across multiple attacks, while previous methods only show robustness against specific attacks. For instance, the Noise method resists geometric transformations like cropping and rotation but fails against Gaussian noise or JPEG compression. Our method’s robustness stems from frequency-domain compression, which discards high-frequency information, embedding this behavior globally in the spatial domain. This makes it resilient to geometric transformations, noise, compression, and other preprocessing. Similar results are observed on GTSRB, CIFAR100, and VGGFace

datasets, as shown in Figures 18, 19, and 20 of our Appendix.

4.6. Covertness

In practical scenarios, adversaries may use detection mechanisms, such as manual inspection or binary classifiers, to block ownership verification via query samples. To counter this, watermark samples must be highly covert, i.e., visually indistinguishable. Figure 6 compares the visual differences between clean samples and watermark samples using different methods on the CIFAR10 task, as well as the residual between the two after being magnified by three times. Our ComMark method achieves excellent covertness, with differences imperceptible even when residuals are magnified three times. We further quantitatively assess covertness using PSNR, SSIM, and LPIPS metrics, as shown in Table 3. ComMark ranks second across all metrics, closely trailing the MAB method, aligning with the visual results in Figure 6. By discarding high-frequency information during watermark sample construction, our method effectively maintains imperceptible differences between watermark and clean samples. Notably, while BlindMark and MAB are also covert, their robustness proves to be poor, as detailed in previous sections.

4.7. Ablation Study

In this section, we perform ablation experiments to evaluate the impact of loss function designs and hyperparameters on ComMark’s performance, focusing on attack loss, similarity loss, watermark sample rate, and compression quality

Table 4. Different watermark success rate (WSR) performances (%) of our watermarking method when resisting watermark evasion attacks and reducing false watermark triggering with (w/) and without (w/o) attack loss L_{attk} .

Method	Resisting Watermark Evasion Attacks (WSR↑)								Reducing False Watermark Triggering (WSR↓)							
	GTSRB		CIFAR10		CIFAR100		VGGFace		GTSRB		CIFAR10		CIFAR100		VGGFace	
	w/o	w/	w/o	w/	w/o	w/	w/o	w/	w/o	w/	w/o	w/	w/o	w/	w/o	w/
Cropping	98.59	99.93	98.72	99.88	99.63	99.95	99.59	99.92	7.72	6.58	17.26	10.33	1.87	1.05	5.38	1.75
Rotation	99.75	99.86	99.23	99.98	99.53	99.98	99.66	99.95	12.38	8.24	12.98	9.71	1.68	1.32	5.60	2.37
Scaling	99.23	99.65	98.32	99.99	99.35	100.00	99.67	99.97	7.10	4.35	13.35	10.09	1.54	0.89	1.69	1.55
Brightness	99.23	99.92	92.68	100.00	99.01	100.00	99.49	100.00	17.82	12.37	15.97	9.70	14.46	1.08	12.95	4.17
Noise	99.90	99.90	99.83	100.00	99.97	100.00	99.93	100.00	24.32	12.53	29.91	9.67	22.31	1.14	25.78	3.68
Blur	97.85	99.39	83.19	98.77	88.95	99.76	99.35	99.73	7.97	4.29	15.74	10.33	1.26	0.88	1.14	0.80
Image Quant.	100.00	100.00	100.00	100.00	100.00	100.00	100.00	100.00	31.54	5.03	34.94	16.49	7.40	3.67	18.52	13.03
Color Quant.	100.00	100.00	99.91	100.00	99.05	99.93	99.89	100.00	19.87	12.33	16.23	9.81	3.57	0.93	3.94	1.74
JPEG2000	95.83	97.79	82.59	95.30	97.33	98.46	78.50	94.54	33.16	14.43	34.98	14.50	25.97	9.30	25.23	7.34
WEBP	88.35	99.04	55.79	88.56	58.26	93.36	69.05	92.72	34.93	15.05	27.96	18.99	26.49	8.13	34.47	12.23

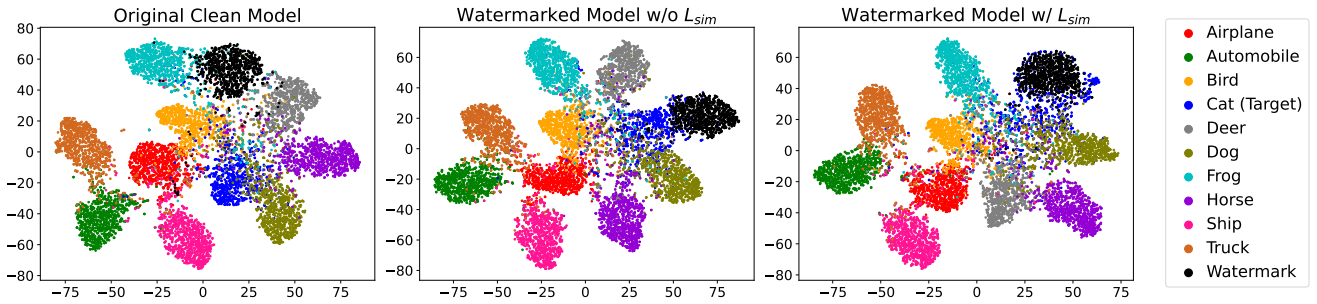


Figure 7. Visualization of t-SNE in the feature space of models with (w/) and without (w/o) similarity loss L_{sim} .

factor. Due to space limitation, results for the latter two are detailed in Table 15 and Table 16 of our Appendix.

4.7.1. Effect of Attack Loss

We first evaluate the impact of attack loss, which generates attacked samples during training. The left half of Table 4 shows robustness against watermark evasion attacks, with attack loss improving watermark success rates by 0% to 36%, depending on the attack type. The right half of Table 4 indicates that attack loss reduces false triggering success rates by 0% to 27%. Overall, our method already exhibits strong resilience to watermark evasion attacks and false triggering, and attack loss further enhances these properties. It should be clear that, unlike watermark evasion attack where an adversary processes the defender’s watermark samples to prevent ownership verification, false triggering is where an adversary uses some data processing techniques to try to forge watermark samples to cause ownership ambiguity.

4.7.2. Effect of Similarity Loss

Our similarity loss has two key goals: enhancing entanglement between watermark samples and target class samples, and stabilizing and accelerating model training. The t-SNE plots [63] in Figure 7 show that similarity loss brings watermark samples closer to target class samples in the representation space, strengthening their correlation and improving watermark robustness. Figure 14 in the Appendix compares

training progress with and without similarity loss, revealing faster convergence, stabilized training, and slight improvements in both model accuracy and watermark success rate when similarity loss is applied.

5. Conclusion

In this paper, we propose a novel watermarking approach using covert behavioral patterns as watermark triggers. Specifically, we introduce a black-box method based on frequency-domain compression, where high-frequency information is discarded through quantization to create covert watermark samples. This global compression behavior, when reverted to the spatial domain, enhances resistance to removal. Additionally, we employ two optimization techniques during training: attack simulation, which improves resistance to attacks and reduces false triggering, and similarity loss, which enhances robustness and stabilizes training by clustering features of same-label samples. Extensive experiments across diverse tasks and datasets demonstrate our method’s superior covertness and robustness. We hope this work will help model owners protect their intellectual property.

References

- [1] Yossi Adi, Carsten Baum, Moustapha Cisse, Benny Pinkas, and Joseph Keshet. Turning your weakness into a strength: Watermarking deep neural networks by backdooring. In 27th

USENIX security symposium (USENIX Security 18), pages 1615–1631, 2018. 1, 2, 5

[2] Nasir Ahmed, T. Natarajan, and Kamisetty R Rao. Discrete cosine transform. *IEEE transactions on Computers*, 100(1): 90–93, 2006. 3

[3] Ronit Akharya. News-topic-classification. <https://github.com/Ronit33/agnews-pytorch-lstm>, 2023. 5

[4] Muzahir Shaban Al-Ani and Fouad Hammadi Awad. The jpeg image compression algorithm. *Int. J. Adv. Eng. Technol.*, 6 (3):1055–1062, 2013. 2

[5] Mahbubul Alam, Manar D Samad, Lasitha Vidyaratne, Alexander Glandon, and Khan M Iftekharuddin. Survey on deep neural networks in speech and vision systems. *Neurocomputing*, 417:302–321, 2020. 1

[6] Abdulsalam Alkholidi, Ayman Alfalou, and Habib Hamam. A new approach for optical colored image compression using the jpeg standards. *Signal Processing*, 87(4):569–583, 2007. 2

[7] Masayuki Asahara and Yuji Matsumoto. Extended models and tools for high-performance part-of-speech. In *COLING 2000 Volume 1: The 18th International Conference on Computational Linguistics*, 2000. 5

[8] The Authors. Source code. <https://github.com/yangyunfei16/ComMark>, 2025. 2

[9] Lennart Behme, Saravanan Thirumuruganathan, Alireza Rezaei Mahdiraji, Jorge-Arnulfo Quiñané-Ruiz, and Volker Markl. The art of losing to win: Using lossy image compression to improve data loading in deep learning pipelines. In *2023 IEEE 39th International Conference on Data Engineering (ICDE)*, pages 936–949. IEEE, 2023. 2

[10] Neelanjan Bhowmik, Jack W Barker, Yona Falimic A Gaus, and Toby P Breckon. Lost in compression: the impact of lossy image compression on variable size object detection within infrared imagery. In *Proceedings of the IEEE/CVF Conference on Computer Vision and Pattern Recognition*, pages 369–378, 2022. 2

[11] Franziska Boenisch. A systematic review on model watermarking for neural networks. *Frontiers in big Data*, 4: 729663, 2021. 1

[12] Karlheinz Brandenburg. Mp3 and aac explained. In *Audio Engineering Society Conference: 17th International Conference: High-Quality Audio Coding*. Audio Engineering Society, 1999. 5

[13] Markus M Breunig, Hans-Peter Kriegel, Raymond T Ng, and Jörg Sander. Lof: identifying density-based local outliers. In *SIGMOD*, 2000. 2

[14] Shilv Cai, Liqun Chen, Sheng Zhong, Luxin Yan, Jiahuan Zhou, and Xu Zou. Make lossy compression meaningful for low-light images. In *Proceedings of the AAAI Conference on Artificial Intelligence*, pages 8236–8245, 2024. 2

[15] Yihan Cao, Siyu Li, Yixin Liu, Zhiling Yan, Yutong Dai, Philip Yu, and Lichao Sun. A survey of ai-generated content (aigc). *ACM Computing Surveys*, 57(5):1–38, 2025. 1

[16] Chin-Chen Chang, Tung-Shou Chen, and Lou-Zo Chung. A steganographic method based upon jpeg and quantization table modification. *Information Sciences*, 141(1-2):123–138, 2002. 2

[17] Huili Chen, Bita Darvish Rouhani, Cheng Fu, Jishen Zhao, and Farinaz Koushanfar. Deepmarks: A secure fingerprinting framework for digital rights management of deep learning models. In *Proceedings of the 2019 on International Conference on Multimedia Retrieval*, pages 105–113, 2019. 2

[18] Li Chen, Penghao Wu, Kashyap Chitta, Bernhard Jaeger, Andreas Geiger, and Hongyang Li. End-to-end autonomous driving: Challenges and frontiers. *IEEE Transactions on Pattern Analysis and Machine Intelligence*, 2024. 1

[19] Francisco F Cunha, Valentin Blüml, Lydia M Zopf, Andreas Walter, Michael Wagner, Wolfgang J Weninger, Lucas A Thomaz, Luís MN Tavora, Luis A da Silva Cruz, and Sergio MM Faria. Lossy image compression in a preclinical multimodal imaging study. *Journal of Digital Imaging*, 36 (4):1826–1850, 2023. 2

[20] Wei Dai, Chia Dai, Shuhui Qu, Juncheng Li, and Samarjit Das. Very deep convolutional neural networks for raw waveforms. In *ICASSP*, 2017. 4

[21] Qiuyu Duan, Zhongyun Hua, Qing Liao, Yushu Zhang, and Leo Yu Zhang. Conditional backdoor attack via jpeg compression. In *Proceedings of the AAAI Conference on Artificial Intelligence*, pages 19823–19831, 2024. 2

[22] Benjamin Dwumah. Image-caption. <https://github.com/Ben74x/Image-Captioning-on-MSCoco-Dataset>, 2022. 5

[23] Raia Hadsell, Sumit Chopra, and Yann LeCun. Dimensionality reduction by learning an invariant mapping. In *2006 IEEE computer society conference on computer vision and pattern recognition (CVPR'06)*, pages 1735–1742. IEEE, 2006. 4

[24] Kaiming He, Xiangyu Zhang, Shaoqing Ren, and Jian Sun. Deep residual learning for image recognition. In *Proceedings of the IEEE conference on computer vision and pattern recognition*, pages 770–778, 2016. 5

[25] Geoffrey Hinton, Oriol Vinyals, and Jeff Dean. Distilling the knowledge in a neural network. *arXiv preprint arXiv:1503.02531*, 2015. 6, 1

[26] Ruitao Hou, Teng Huang, Hongyang Yan, Lishan Ke, and Weixuan Tang. A stealthy and robust backdoor attack via frequency domain transform. *World Wide Web*, 26(5):2767–2783, 2023. 2

[27] Quan Huynh-Thu and Mohammed Ghanbari. Scope of validity of psnr in image/video quality assessment. *Electronics letters*, 44(13):800–801, 2008. 5

[28] Hengrui Jia, Christopher A Choquette-Choo, Varun Chandrasekaran, and Nicolas Papernot. Entangled watermarks as a defense against model extraction. In *30th USENIX security symposium (USENIX Security 21)*, pages 1937–1954, 2021. 1, 6

[29] Byungjoo Kim, Suyoung Lee, Seanie Lee, Sooel Son, and Sung Ju Hwang. Margin-based neural network watermarking. In *International Conference on Machine Learning*, pages 16696–16711. PMLR, 2023. 1, 2, 5

[30] Lingshun Kong, Jiangxin Dong, Jianjun Ge, Mingqiang Li, and Jinshan Pan. Efficient frequency domain-based transformers for high-quality image deblurring. In *Proceedings of the IEEE/CVF Conference on Computer Vision and Pattern Recognition*, pages 5886–5895, 2023. 2

[31] Jesse D Kornblum. Using jpeg quantization tables to identify imagery processed by software. *digital investigation*, 5:S21–S25, 2008. 4

[32] Alex Krizhevsky, Geoffrey Hinton, et al. Learning multiple layers of features from tiny images. 2009. 5

[33] Lamyanba Laishram, Muhammad Shaheryar, Jong Taek Lee, and Soon Ki Jung. Toward a privacy-preserving face recognition system: A survey of leakages and solutions. *ACM Computing Surveys*, 57(6):1–38, 2025. 1

[34] Peixuan Li, Pengzhou Cheng, Fangqi Li, Wei Du, Haodong Zhao, and Gongshen Liu. Plmmark: a secure and robust black-box watermarking framework for pre-trained language models. In *Proceedings of the AAAI Conference on Artificial Intelligence*, pages 14991–14999, 2023. 2

[35] Zheng Li, Chengyu Hu, Yang Zhang, and Shanqing Guo. How to prove your model belongs to you: A blind-watermark based framework to protect intellectual property of dnn. In *Proceedings of the 35th annual computer security applications conference*, pages 126–137, 2019. 1, 2, 5

[36] Tsung-Yi Lin, Michael Maire, Serge Belongie, James Hays, Pietro Perona, Deva Ramanan, Piotr Dollár, and C Lawrence Zitnick. Microsoft coco: Common objects in context. In *ECCV*, 2014. 5

[37] Fei Tony Liu, Kai Ming Ting, and Zhi-Hua Zhou. Isolation forest. In *ICDM*, 2008. 2

[38] Yuyang Long, Qilong Zhang, Boheng Zeng, Lianli Gao, Xianglong Liu, Jian Zhang, and Jingkuan Song. Frequency domain model augmentation for adversarial attack. In *European conference on computer vision*, pages 549–566. Springer, 2022. 2

[39] Nils Lukas, Edward Jiang, Xinda Li, and Florian Ker-schbaum. Sok: How robust is image classification deep neural network watermarking? In *S&P*, 2022. 7, 2

[40] Peizhuo Lv, Pan Li, Shencheng Zhu, Shengzhi Zhang, Kai Chen, Ruigang Liang, Chang Yue, Fan Xiang, Yuling Cai, Hualong Ma, et al. Ssl-wm: A black-box watermarking approach for encoders pre-trained by self-supervised learning. *arXiv preprint arXiv:2209.03563*, 2022. 2

[41] Peizhuo Lv, Pan Li, Shengzhi Zhang, Kai Chen, Ruigang Liang, Hualong Ma, Yue Zhao, and Yingjiu Li. A robustness-assured white-box watermark in neural networks. *IEEE Transactions on Dependable and Secure Computing*, 20(6):5214–5229, 2023. 1

[42] Peizhuo Lv, Hualong Ma, Kai Chen, Jiachen Zhou, Shengzhi Zhang, Ruigang Liang, Shencheng Zhu, Pan Li, and Yingjun Zhang. Mea-defender: a robust watermark against model extraction attack. In *2024 IEEE Symposium on Security and Privacy (SP)*, pages 2515–2533. IEEE, 2024. 1, 2, 5, 6, 3

[43] Andrew Maas, Raymond E Daly, Peter T Pham, Dan Huang, Andrew Y Ng, and Christopher Potts. Learning word vectors for sentiment analysis. In *Proceedings of the 49th annual meeting of the association for computational linguistics: Human language technologies*, pages 142–150, 2011. 5

[44] Cao Mi. Audio-scene-classification. <https://github.com/caomi8888/pytorch-for-Audio-Classification>, 2024. 5

[45] Ryota Namba and Jun Sakuma. Robust watermarking of neural network with exponential weighting. In *Proceedings of the 2019 ACM Asia Conference on Computer and Communications Security*, pages 228–240, 2019. 2

[46] Hewang Nie and Songfeng Lu. Fedcrmw: Federated model ownership verification with compression-resistant model watermarking. *Expert Systems with Applications*, 249:123776, 2024. 2

[47] Hewang Nie, Songfeng Lu, Junjun Wu, and Jianxin Zhu. Deep model intellectual property protection with compression-resistant model watermarking. *IEEE Transactions on Artificial Intelligence*, 5(7):3362–3373, 2024. 1

[48] Tribhuvanesh Orekondy, Bernt Schiele, and Mario Fritz. Knockoff nets: Stealing functionality of black-box models. In *Proceedings of the IEEE/CVF conference on computer vision and pattern recognition*, pages 4954–4963, 2019. 6, 1

[49] Kaiyi Pang, Tao Qi, Chuhan Wu, Minhao Bai, Minghu Jiang, and Yongfeng Huang. Modelshield: Adaptive and robust watermark against model extraction attack. *IEEE Transactions on Information Forensics and Security*, 2025. 2

[50] Nicolas Papernot, Patrick McDaniel, Ian Goodfellow, Somesh Jha, Z Berkay Celik, and Ananthram Swami. Practical black-box attacks against machine learning. In *Proceedings of the 2017 ACM on Asia conference on computer and communications security*, pages 506–519, 2017. 6, 1

[51] Omkar Parkhi, Andrea Vedaldi, and Andrew Zisserman. Deep face recognition. In *BMVC 2015-Proceedings of the British Machine Vision Conference 2015*. British Machine Vision Association, 2015. 5

[52] Alec Radford, Jeffrey Wu, Rewon Child, David Luan, Dario Amodei, Ilya Sutskever, et al. Language models are unsupervised multitask learners. *OpenAI blog*, 2019. 5

[53] Iain E Richardson. *H. 264 and MPEG-4 video compression: video coding for next-generation multimedia*. John Wiley & Sons, 2004. 5

[54] Justin Salamon, Christopher Jacoby, and Juan Pablo Bello. A dataset and taxonomy for urban sound research. In *Proceedings of the 22nd ACM international conference on Multimedia*, pages 1041–1044, 2014. 5

[55] Wojciech Samek, Grégoire Montavon, Sebastian Lapuschkin, Christopher J Anders, and Klaus-Robert Müller. Explaining deep neural networks and beyond: A review of methods and applications. *Proceedings of the IEEE*, 109(3):247–278, 2021. 1

[56] Khurram Soomro, Amir Roshan Zamir, and Mubarak Shah. Ucf101: A dataset of 101 human actions classes from videos in the wild. *arXiv preprint arXiv:1212.0402*, 2012. 5

[57] Taarun Srinivas. Image-generation. <https://github.com/Taarun-Srinivas/Fashion-MNIST-classification-using-autoencoders>, 2023. 5

[58] Johannes Stallkamp, Marc Schlipsing, Jan Salmen, and Christian Igel. The german traffic sign recognition benchmark: a multi-class classification competition. In *The 2011 international joint conference on neural networks*, pages 1453–1460. IEEE, 2011. 4

[59] Vivienne Sze, Yu-Hsin Chen, Tien-Ju Yang, and Joel S Emer. Efficient processing of deep neural networks: A tutorial and

survey. *Proceedings of the IEEE*, 105(12):2295–2329, 2017. 1

[60] Jingxuan Tan, Nan Zhong, Zhenxing Qian, Xinpeng Zhang, and Sheng Li. Deep neural network watermarking against model extraction attack. In *Proceedings of the 31st ACM international conference on multimedia*, pages 1588–1597, 2023. 1, 6

[61] Ruixiang Tang, Hongye Jin, Mengnan Du, Curtis Wigington, Rajiv Jain, and Xia Hu. Exposing model theft: A robust and transferable watermark for thwarting model extraction attacks. In *Proceedings of the 32nd ACM International Conference on Information and Knowledge Management*, pages 4315–4319, 2023. 6

[62] Yusuke Uchida, Yuki Nagai, Shigeyuki Sakazawa, and Shin’ichi Satoh. Embedding watermarks into deep neural networks. In *Proceedings of the 2017 ACM on international conference on multimedia retrieval*, pages 269–277, 2017. 2

[63] Laurens Van der Maaten and Geoffrey Hinton. Visualizing data using t-sne. *JMLR*, 2008. 8

[64] Gregory K Wallace. The jpeg still picture compression standard. *Communications of the ACM*, 34(4):30–44, 1991. 2, 5

[65] Wenbo Wan, Jun Wang, Yunming Zhang, Jing Li, Hui Yu, and Jiande Sun. A comprehensive survey on robust image watermarking. *Neurocomputing*, 488:226–247, 2022. 1

[66] Tianhao Wang and Florian Kerschbaum. Riga: Covert and robust white-box watermarking of deep neural networks. In *Proceedings of the web conference 2021*, pages 993–1004, 2021. 1

[67] Zhou Wang, Alan C Bovik, Hamid R Sheikh, and Eero P Simoncelli. Image quality assessment: from error visibility to structural similarity. *IEEE transactions on image processing*, 13(4):600–612, 2004. 5

[68] Pete Warden. Speech commands: A dataset for limited-vocabulary speech recognition. *arXiv:1804.03209*, 2018. 4

[69] Shaowu Wu, Wei Lu, Xiaolin Yin, and Rui Yang. Robust watermarking against arbitrary scaling and cropping attacks. *Signal Processing*, 226:109655, 2025. 2

[70] Zuping Xi, Zuomin Qu, Wei Lu, Xiangyang Luo, and Xiaochun Cao. Invisible dnn watermarking against model extraction attack. *IEEE Transactions on Cybernetics*, 2024. 1

[71] Han Xiao, Kashif Rasul, and Roland Vollgraf. Fashion-mnist: a novel image dataset for benchmarking machine learning algorithms. *arXiv:1708.07747*, 2017. 5

[72] Yifan Yan, Xudong Pan, Mi Zhang, and Min Yang. Rethinking {White-Box} watermarks on deep learning models under neural structural obfuscation. In *32nd USENIX Security Symposium (USENIX Security 23)*, pages 2347–2364, 2023. 1

[73] Sze Jue Yang, Quang Nguyen, Chee Seng Chan, and Khoa D Doan. Everyone can attack: Repurpose lossy compression as a natural backdoor attack. *arXiv preprint arXiv:2308.16684*, 2023. 2

[74] Chang Yue, Peizhuo Lv, Ruigang Liang, and Kai Chen. Invisible backdoor attacks using data poisoning in frequency domain. In *ECAI 2023*, pages 2954–2961. IOS Press, 2023. 2

[75] Jianfeng Zhang. Video-action-recognition. <https://github.com/jfzhang95/pytorch-video-recognition>, 2018. 5

[76] Jialong Zhang, Zhongshu Gu, Jiyong Jang, Hui Wu, Marc Ph Stoecklin, Heqing Huang, and Ian Molloy. Protecting intellectual property of deep neural networks with watermarking. In *Proceedings of the 2018 on Asia conference on computer and communications security*, pages 159–172, 2018. 1, 2, 5

[77] Jie Zhang, Dongdong Chen, Jing Liao, Han Fang, Weiming Zhang, Wenbo Zhou, Hao Cui, and Nenghai Yu. Model watermarking for image processing networks. In *Proceedings of the AAAI conference on artificial intelligence*, pages 12805–12812, 2020. 1

[78] Jie Zhang, Dongdong Chen, Jing Liao, Weiming Zhang, Huamin Feng, Gang Hua, and Nenghai Yu. Deep model intellectual property protection via deep watermarking. *IEEE Transactions on Pattern Analysis and Machine Intelligence*, 44(8):4005–4020, 2021. 1

[79] Richard Zhang, Phillip Isola, Alexei A Efros, Eli Shechtman, and Oliver Wang. The unreasonable effectiveness of deep features as a perceptual metric. In *Proceedings of the IEEE conference on computer vision and pattern recognition*, pages 586–595, 2018. 5

[80] Xiang Zhang, Junbo Zhao, and Yann LeCun. Character-level convolutional networks for text classification. *NeurIPS*, 2015. 5

[81] Yijie Zhong, Bo Li, Lv Tang, Senyun Kuang, Shuang Wu, and Shouhong Ding. Detecting camouflaged object in frequency domain. In *Proceedings of the IEEE/CVF conference on computer vision and pattern recognition*, pages 4504–4513, 2022. 2

[82] Hongyu Zhu, Sichu Liang, Wentao Hu, Li Fangqi, Ju Jia, and Shi-Lin Wang. Reliable model watermarking: Defending against theft without compromising on evasion. In *Proceedings of the 32nd ACM International Conference on Multimedia*, pages 10124–10133, 2024. 1

ComMark: Covert and Robust Black-Box Model Watermarking with Compressed Samples

Supplementary Material

Table 5. Comparison of robustness (%) against cross-dataset extraction attacks. The primary task is CIFAR10.

Method	Query Set of Adversary							
	CIFAR10		CIFAR100		GTSRB		VGGFace	
	Acc	WSR↑	Acc	WSR↑	Acc	WSR↑	Acc	WSR↑
Abstract	65.13	72.00	43.31	74.00	16.55	33.00	11.08	16.00
Content	36.35	9.23	53.13	21.09	17.92	56.45	15.58	74.57
MEAD	50.94	95.36	35.74	96.88	17.96	62.04	17.18	67.38
Noise	61.80	14.06	57.67	15.47	16.33	39.80	15.95	52.83
BlindMark	51.21	17.40	32.33	18.20	14.50	9.60	16.60	12.40
MAB	66.23	12.40	46.79	12.60	14.14	8.00	16.29	11.20
ComMark	77.57	98.13	72.32	98.93	22.91	69.09	28.41	71.42

Table 6. Comparison of robustness (%) against cross-architecture extraction attacks. The model architecture of victim is ResNet18.

Method	Model Architecture of Adversary							
	ResNet18		ResNet34		VGG16		AlexNet	
	Acc	WSR↑	Acc	WSR↑	Acc	WSR↑	Acc	WSR↑
Abstract	65.13	72.00	44.66	34.00	10.00	10.00	27.13	36.00
Content	36.35	9.23	51.02	10.77	18.97	1.54	29.15	19.27
MEAD	50.94	95.36	28.50	90.80	19.78	67.19	19.58	71.94
Noise	61.80	14.06	53.42	6.42	10.00	52.06	30.53	9.12
BlindMark	51.21	17.40	62.09	19.00	28.72	13.20	36.59	12.60
MAB	66.23	12.40	58.99	13.60	10.00	11.00	23.86	6.40
ComMark	88.12	98.13	75.59	92.85	27.55	76.81	31.83	82.49

Table 7. Comparison of robustness (%) against cross-dataset and cross-architecture extraction attacks. The victim model is ResNet18 trained on CIFAR10.

Method	Query Set and Model Architecture of Adversary							
	CIFAR100		GTSRB		VGGFace		TinyImageNet	
	VGG16		AlexNet		ResNet34		DenseNet161	
	Acc	WSR↑	Acc	WSR↑	Acc	WSR↑	Acc	WSR↑
Abstract	10.00	10.00	14.14	19.00	10.43	10.00	23.20	88.00
Content	14.44	6.60	11.13	0.64	14.18	84.47	37.02	3.22
MEAD	19.49	98.43	11.34	46.91	12.54	79.83	17.16	99.74
Noise	10.00	94.96	12.46	13.25	19.35	67.90	36.79	14.85
BlindMark	18.67	11.80	12.03	9.80	11.27	11.40	20.94	13.20
MAB	10.00	11.00	10.65	9.80	16.65	10.40	36.97	13.00
ComMark	17.74	97.61	14.27	53.11	20.91	83.27	39.14	99.59

A. More Evaluation of Robustness against Model Extraction Attacks

We briefly introduce the key ideas of popular extraction attacks here.

• Distillation [25]: This attack removes the hard loss term from the standard KL-divergence-based knowledge distillation loss, retaining only the soft loss term. In this scenario, the adversary has access to the original or simi-

larly distributed primary task training data, and can query the victim model using these data while constraining the outputs of the victim and extracted models to be similar using KL divergence loss.

• JBDA [50]: The adversary has access to a small set of original training data (seed samples) as the initial query set, and at each epoch, they expand the query set using Jacobian-based data augmentation technique for model extraction attack.

• Knockoff [48]: The adversary can only access publicly available substitute data for model queries. To improve query efficiency, the adversary uses a reinforcement learning strategy to construct a transfer set from a large pool of public data for the attack.

• Hard-Label: The three attack methods described above all operate in scenarios where the victim model outputs soft-label results. We adapt them to the hard-label output scenario to form three new attacks.

• Cross-Dataset: The adversary uses a query dataset with a different distribution from the victim’s training set to perform the Knockoff attack.

• Cross-Architecture: The adversary uses an extracted model with a different model architecture from the victim model for the Knockoff attack.

• Cross-Dataset and Cross-Architecture: In this more challenging scenario, the adversary uses both a query dataset with a different distribution and an extracted model with a different architecture compared to the victim’s.

A.2. More Results

The results in Table 5, Table 6 and Table 7 demonstrate the superior robustness of our proposed watermarking method even when it encounters the three challenging model extraction attacks, namely Cross-Dataset, Cross-Architecture, Cross-Dataset & Cross-Architecture, respectively.

B. More Evaluation of Robustness against Watermark Removal Attacks

B.1. Watermark Removal Attacks

The principles of these attacks are as follows:

• Finetuning [1]: The adversary finetunes the watermarked model using a subset of labeled training data, but only updates the parameters of some layers of the network. In our evaluation, we finetune for 100 epochs and update only the parameters of the last layer.

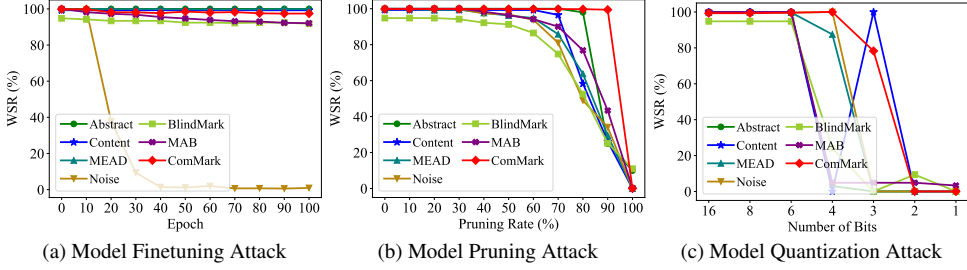


Figure 8. Comparison of robustness against watermark removal attacks. (On GTSRB)

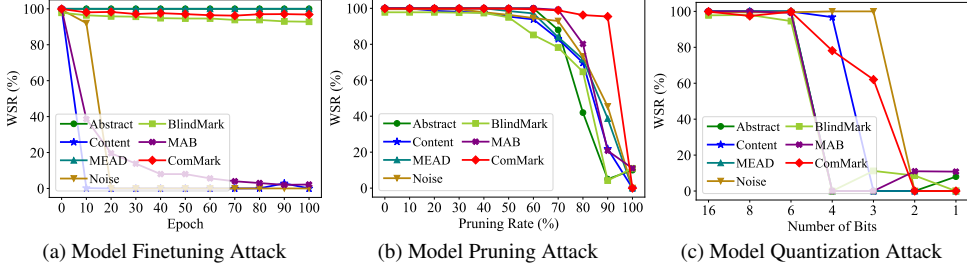


Figure 9. Comparison of robustness against watermark removal attacks. (On CIFAR100)

- Pruning [62]: The adversary prunes a certain proportion of the smallest network weights and sets them to zero. We vary the pruning rate from 0% to 100%.

- Quantization [39]: The adversary compresses all weights of the network into a lower bit representation to save storage resources. We decrease the number of bit from 16 to 1.

B.2. More Results

Figure 8, Figure 9 and Figure 10 show the results of our watermarking approach to resist removal attacks on three tasks, GTSRB, CIFAR100 and VGGFace, respectively. It can be seen that our embedded watermark is more difficult to be erased by current popular watermark removal attacks compared to previous black-box methods. Overall, our method has better robustness.

C. Covertness against Watermark Detection Attacks

In addition to demonstrating the covertness of our method through visual residuals and image similarity in the previous section, we now evaluate the covertness of various watermarking methods against watermark detection attacks. We adopt two popular anomaly detection methods, Local Outlier Factor (LOF) [13] and Isolation Forest (IF) [37], to assess the covertness of watermarks. LOF identifies local outliers by comparing the density differences between data points and their neighbors, considering points with large density differences as anomalies. IF isolates data points by

Table 8. Comparison of covertness (%) against watermark detection attacks. AccLoss, FP, and DetW are abbreviations for the metrics Accuracy Loss, False Positive, and Detected Watermark, respectively.

Dataset	Method	LOF			IF		
		AccLoss	FP	DetW \downarrow	AccLoss	FP	DetW \downarrow
GTSRB	Abstract	13.98	14.73	0.00	12.55	13.46	0.00
	Content	13.91	14.73	0.00	12.71	13.46	0.00
	MEAD	13.91	14.73	29.17	12.89	13.46	10.69
	Noise	13.99	14.73	0.00	12.66	13.46	0.00
	BlindMark	13.86	14.77	1.00	12.42	13.45	0.00
	MAB	13.96	14.73	11.73	12.76	13.46	10.71
CIFAR10	ComMark	13.69	14.73	0.00	12.29	13.46	0.00
	Abstract	8.53	10.22	0.00	10.94	13.43	0.00
	Content	8.53	10.22	9.99	10.88	13.43	12.13
	MEAD	8.49	10.22	0.00	10.85	13.43	0.00
	Noise	8.35	10.22	10.27	10.81	13.43	13.33
	BlindMark	8.30	10.22	0.00	10.76	13.43	0.00
CIFAR100	MAB	8.45	10.22	9.80	10.97	13.43	13.40
	ComMark	8.13	10.22	0.00	10.60	13.43	0.00
	Abstract	5.66	7.64	0.00	9.58	12.30	0.00
	Content	5.47	7.64	7.23	9.25	12.30	11.61
	MEAD	5.38	7.64	0.00	9.22	12.30	0.00
	Noise	5.54	7.64	7.50	9.22	12.30	11.97
VGGFace	BlindMark	5.60	7.64	0.00	9.21	12.30	0.00
	MAB	5.56	7.64	9.80	9.29	12.30	14.40
	ComMark	5.23	7.64	0.00	9.02	12.30	0.00
	Abstract	7.40	18.81	0.00	7.74	20.68	0.00
	Content	7.04	18.81	0.00	7.38	20.68	0.00
	MEAD	7.35	18.81	46.00	7.90	20.68	36.00
VGGFace	Noise	6.93	18.81	0.00	7.51	20.68	0.00
	BlindMark	7.13	18.81	0.00	7.66	20.68	0.40
	MAB	7.35	18.81	13.10	7.85	20.68	12.30
	ComMark	6.95	18.81	0.00	7.46	20.68	0.00

constructing multiple random trees, where points that are harder to isolate are considered anomalous.

The watermark detection results are shown in Table 8. It

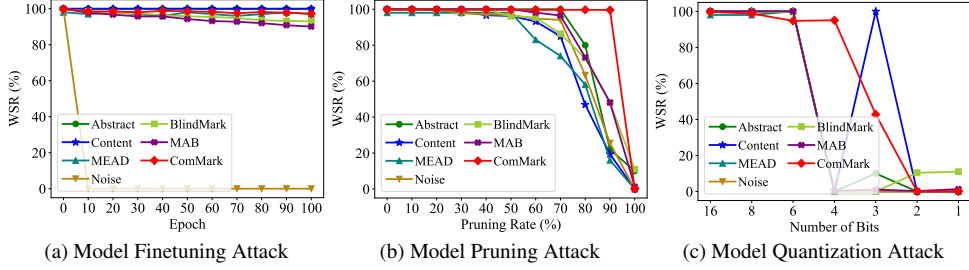


Figure 10. Comparison of robustness against watermark removal attacks. (On VGGFace)

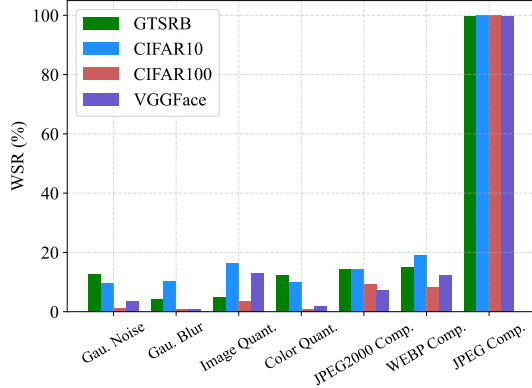


Figure 11. Resistance to false watermark triggering conditions.

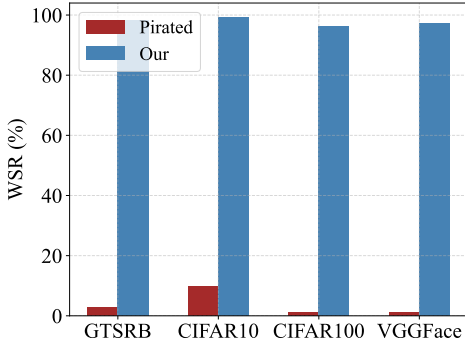


Figure 12. Resistance to watermark ambiguity attacks.

can be seen that while maintaining an acceptable loss in primary task accuracy and false positive rates of clean samples, our watermarking method achieves a 0% watermark detection rate across all datasets and anomaly detection methods, meaning that watermark samples are not detected as anomalous by the respective algorithms. Among previous watermarking methods, only Abstract achieves 0% watermark detection rate across all scenarios, while other methods have some watermark samples detected as anomalous in certain scenarios.

D. Uniqueness

An ideal watermarking method, in addition to having sufficient effectiveness, covertness, and robustness, should also ensure that it is difficult for adversaries to trigger the watermark using other patterns, thereby preventing ownership disputes. We first investigate whether the watermarked model might mistakenly interpret some pixel-level artifacts as watermark triggering conditions. To explore this, we generate watermark samples using data preprocessing operations such as Gaussian Noise, Gaussian Blur, Image Quantization, Color Quantization, JPEG2000 Compression, and WEBP Compression, and test if these could lead to false watermark triggering. The results are shown in Figure 11. We observe that only watermark samples generated using our JPEG Compression are able to trigger the watermark successfully, achieving over 99% watermark success rate, while the success rate for other samples is very low, with the highest being only 18.99%. This indicates that the watermarked model has learned the specific behavior condition of our JPEG compression, rather than pixel-level artifact features.

Additionally, we deploy a strong watermark ambiguity attack [42], where the adversary first uses 20% of the query data to embed their own watermark into the extracted model (with the watermark sample consisting of a fixed-colored square placed at the bottom right corner of clean samples), and then uses the remaining 80% of the query data to perform Knockoff model extraction attack. We then inspect the survival of both the adversary’s watermark and our watermark in the final extracted model. The results in Figure 12 show that our watermark is still successfully verified with a very high success rate, while the adversary’s pre-embedded watermark is easily removed after the model extraction attack.

In conclusion, our unique watermarking approach effectively resists false triggering and watermark ambiguity attacks, providing a stronger black-box technology for model copyright protection.

Table 9. Generalized performance of our watermarking method on various deep learning tasks. In the image generation and image caption tasks, we use SSIM and BLEU-4 metrics for evaluating the model performance, respectively, when the other tasks are evaluated using test accuracy.

Task Domain →	Speech Command Recognition	Audio Scene Classification	Sentiment Analysis	News Topic Classification	Image Generation	Image Caption	Video Action Recognition
Data Modality →	Audio	Audio	Text	Text	Image Fashion MNIST	Image+Text MSCOCO	Video UCF101
Task Dataset →	Speech Commands	UrbanSound8K	IMDB	AG News	Multi-Layer LSTM	AutoEncoder	ResNet50+LSTM C3D
Model Architecture →	M5	VGG-like	GPT2				
Clean Model	Acc WSR	86.14% 2.57%	80.26% 8.90%	89.30% 48.80%	88.82% 24.07%	0.7358 0.2569	0.1599 0.0711
Watermarked Model	Acc WSR	83.04% 99.49%	77.73% 97.82%	88.00% 99.40%	86.96% 96.30%	0.7155 0.9707	0.1512 0.9138
Extracted Model	Acc WSR	80.51% 90.12%	75.39% 91.96%	85.70% 72.70%	85.16% 73.00%	0.7042 0.6831	0.1386 0.7925
Fine-tuned Model	Acc WSR	84.14% 97.52%	81.63% 95.71%	94.40% 86.75%	89.14% 78.89%	0.7289 0.6923	0.1453 0.7915
Watermark Sample vs. Clean Sample	Cosine Similarity	0.9982	0.9905	0.9714	0.9588	0.9950	0.9936
							0.9408

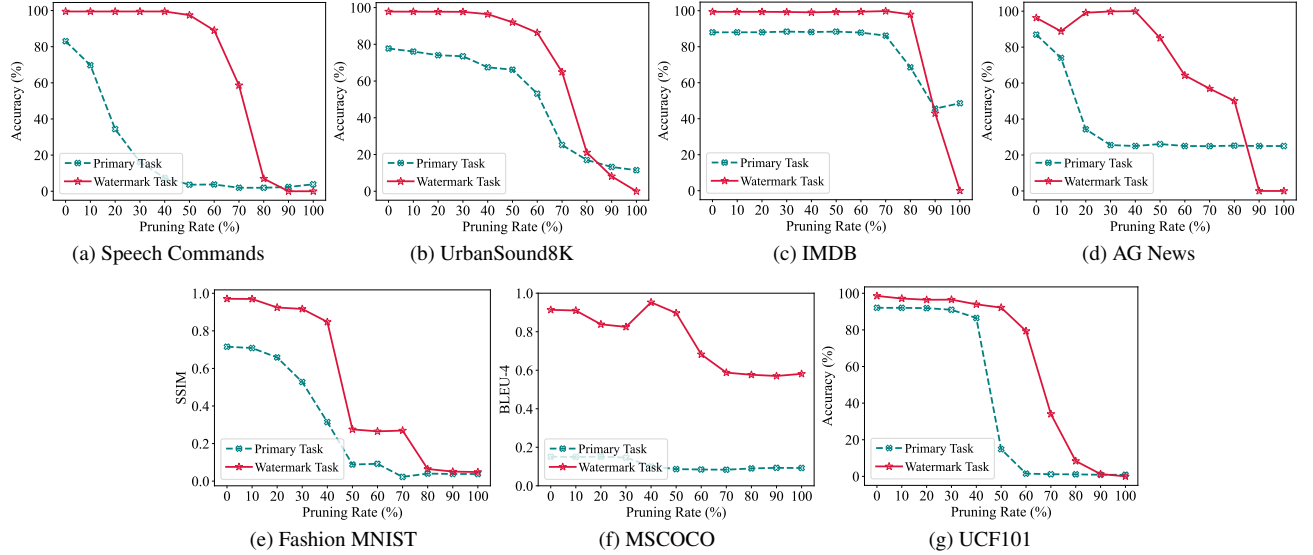


Figure 13. Generalized robustness of our watermarking method against model pruning attacks on various deep learning tasks.

E. Generalizability

Our watermarking method is generalizable and can be extended to various deep learning domains and data modalities. Specifically, when applying our method to tasks beyond image recognition, the main adjustment lies in selecting appropriate compression algorithms for different data modalities to construct the corresponding watermark samples. In this section, we extend our watermarking method to seven deep learning tasks: speech command recognition, audio scene classification, sentiment analysis, news topic classification, image generation, image captioning,

and video action recognition. These tasks encompass four common data modalities: image, audio, video, and text. We first introduce the datasets and models, followed by the watermark sample construction methods for each data modality, and conclude with extensive experimental results.

E.1. Datasets and Models

The introduction of the datasets and models we used in this evaluation is as follows:

- **Speech Commands** [68]: A speech command recognition dataset containing 35 commands spoken by different individuals. The model we use is the M5 model from [20].

- UrbanSound8K [54]: An audio scene classification dataset consisting of 10 different environmental sounds from urban settings. The model we use is the VGG-like architecture (4Conv+1FC) from [44].
- IMDB [43]: A sentiment analysis dataset containing a large collection of movie reviews classified as either positive or negative. We use the pre-trained GPT2 model [52] as the initial architecture.
- AG News [80]: A news topic classification dataset containing four categories: World, Sports, Business, and Sci/Tec. We use a Multi-Layer LSTM [3] as the model architecture.
- Fashion MNIST [71]: A dataset containing 10 categories of grayscale fashion images. This dataset serves as the target for our image generation task, with an AutoEncoder [57] as the generative model.
- MSCOCO [36]: A benchmark image captioning dataset where each image is paired with five different captions describing prominent entities and events. We use this dataset for the multimodal task of image captioning, and employ a model combination [22] of ResNet50 and LSTM.
- UCF101 [56]: A video action recognition dataset consisting of 101 categories of human action video clips. We use C3D model [75], a 3D convolutional neural network designed for video data processing.

E.2. Watermark Sample Construction Methods

Image, audio, and video data are continuous, allowing for transformations from spatial to frequency domains, and there are numerous mature compression algorithms based on frequency domain transformations. Therefore, for these three types of data, we adopt the core steps of the JPEG [64] (image compression), MP3 [12] (audio compression), and H264 [53] (video compression) algorithms to construct watermark samples. Specifically, for these data types, we first preprocess them by converting from the spatial to the frequency domain, then apply quantization-based compression in the frequency domain, and finally perform post-processing to restore the compressed data back to the spatial domain. This results in watermark samples that are both covert and robust, as they discard high-frequency information that is less perceptible to human eye and this discarding behavior is located in the global region of the image in the spatial domain.

However, text data is discrete and unsuitable for frequency-domain compression. To address this, we implement an approximate sample compression method. Specifically, we remove determiners, auxiliary verbs, coordinating conjunctions, and adjectives from the text through part-of-speech analysis [7], and the resulting text becomes the watermark sample. These words typically occupy only a small portion of the text and do not contribute significantly to the semantic core of the text. Therefore, their removal does not

noticeably affect the original meaning, making this a covert form of approximate compression for text data.

E.3. Evaluation Results

Our experimental results are presented in Table 9, which includes the primary task accuracy and watermark success rates for clean models, watermarked models, extracted models, and fine-tuned models across various datasets. The performance of the watermarked models reflects the effectiveness and harmlessness of our method, while the performance of the extracted and fine-tuned models measures the robustness of the watermark. We observe that, even with the addition of our watermarking method, the accuracy drop is only 4.78% on the UCF101 dataset, which has the largest impact on the primary task. Watermark success rates across all datasets exceed 90%. In the case of model extraction attacks, the watermark success rate on the IMDB dataset, which is most severely affected by watermark removal, remains 72.70%. During fine-tuning attacks, the most damaged watermark occurs in the Fashion MNIST image generation task, but it still retains an SSIM value of 0.6923, which is sufficient to assert model ownership. Furthermore, we compute the cosine similarity between clean samples and watermark samples to quantify watermark covertness. The cosine similarities across all datasets exceed 0.94, indicating a high similarity between watermark and original samples.

For robustness evaluation, we also observe the effect of our watermark under model pruning attacks, as shown in Figure 13. We find that only when the pruning rate is very high is our watermark completely removed, at which point the model’s primary task performance is completely lost, rendering the model unusable. Therefore, it is infeasible for an adversary to remove our watermark without affecting model usability.

In summary, all the aforementioned results demonstrate that our method maintains consistently superb effectiveness, harmlessness, robustness, and covertness across different task domains and data modalities, providing strong evidence for the generalizability of our watermarking method.

F. Additional Ablation Studies

F.1. Effect of Watermark Sample Rate

The watermark sample rate refers to the proportion of normal samples that are transformed into watermark samples. In Figure 15, we demonstrate the performance of the watermarked model and its ability to resist evasion attacks and false triggering at different watermark sample rates. We observe that as the watermark sample rate increases, the primary task performance of the watermarked model gradually decreases, while the watermark success rate slightly increases. Meanwhile, the model’s resistance to watermark

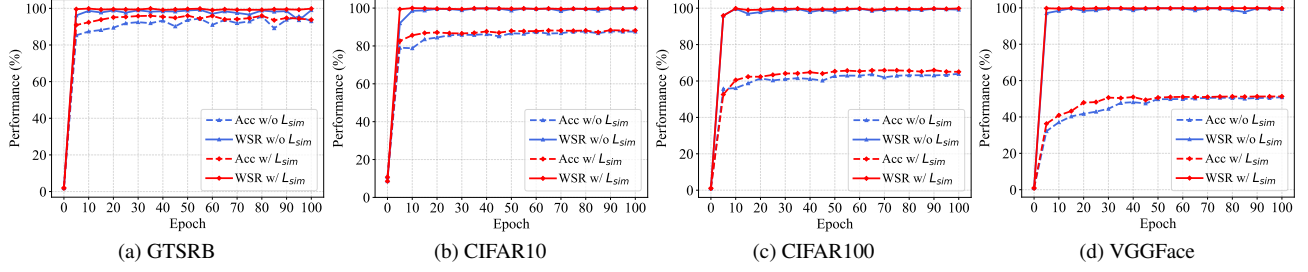


Figure 14. The change in model performance with (w) and without (w/o) similarity loss L_{sim} as the training epochs increase.

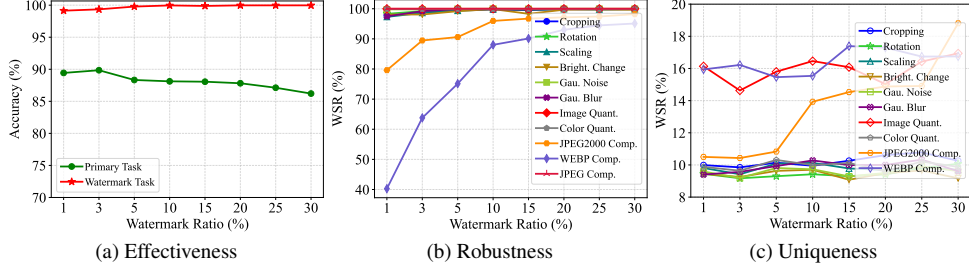


Figure 15. The effect of different watermark sample rates.

evasion attacks improves significantly, with little change in its resistance to false triggering. These trends align with our expectations. Considering the balance between model’s primary task performance and watermark robustness, we ultimately set the watermark sample rate to 10%.

F.2. Effect of Compression Quality Factor

We also evaluate the impact of the JPEG compression quality factor in our watermarking algorithm on the final model performance, as well as its ability to resist evasion attacks and false triggering, with the results summarized in Figure 16. We observe that as the compression quality factor decreases (i.e., as the degree of compression increases), there are no significant changes in the model’s primary task accuracy, watermark success rate, or resistance to evasion attacks and false triggering. These results suggest that even slight compression can successfully embed the watermark, indicating that our watermarked model learns a compression behavior in frequency domain rather than specific pixel-level quantitative changes. A higher compression quality factor leads to a smaller difference between the watermark sample and the original clean sample, and considering covertness, we set the compression quality factor to 90.

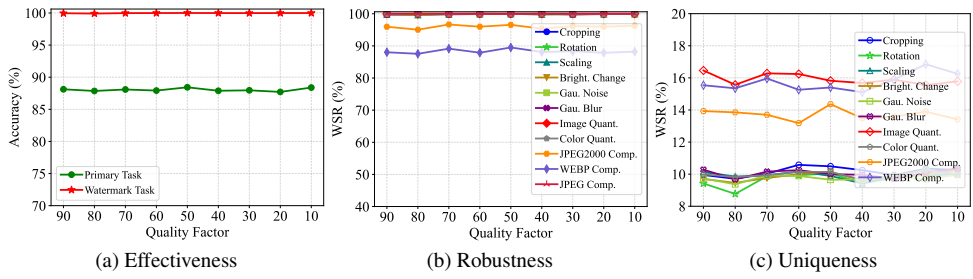


Figure 16. The effect of different compression quality factors.

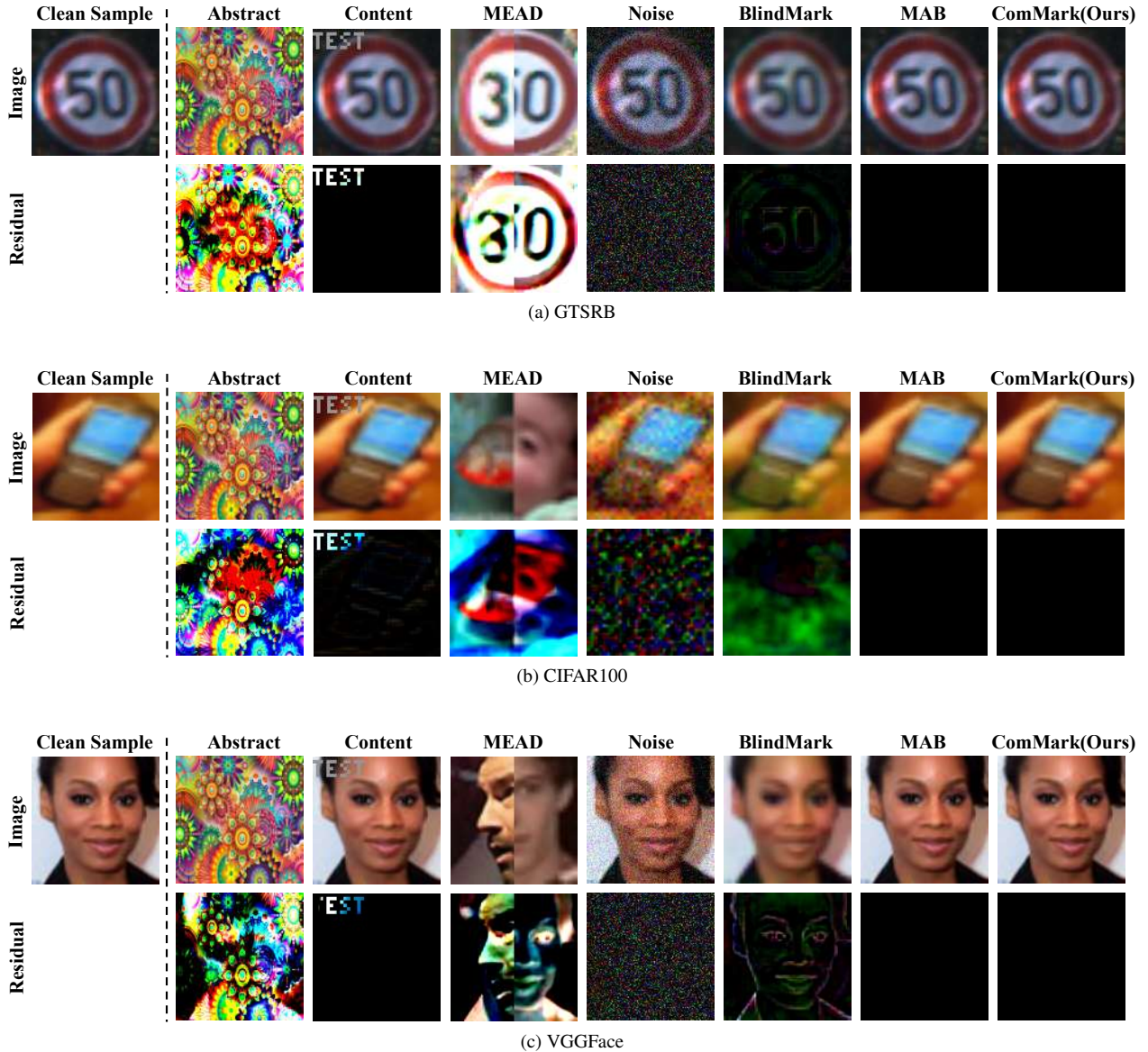


Figure 17. Visual comparison of covertness of different watermarking methods. (On GTSRB, CIFAR100 and VGGFace)

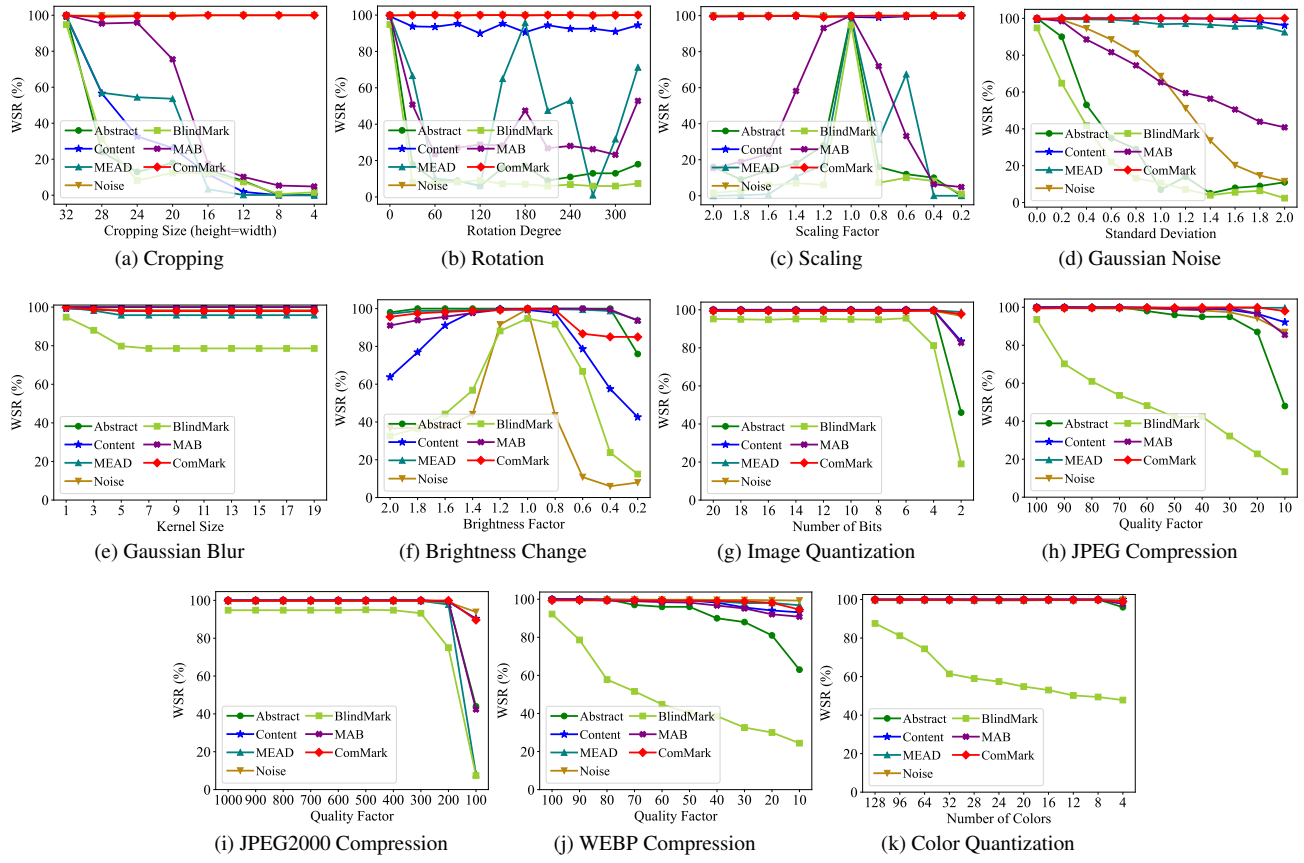


Figure 18. Comparison of robustness against watermark evasion attacks. (On GTSRB)

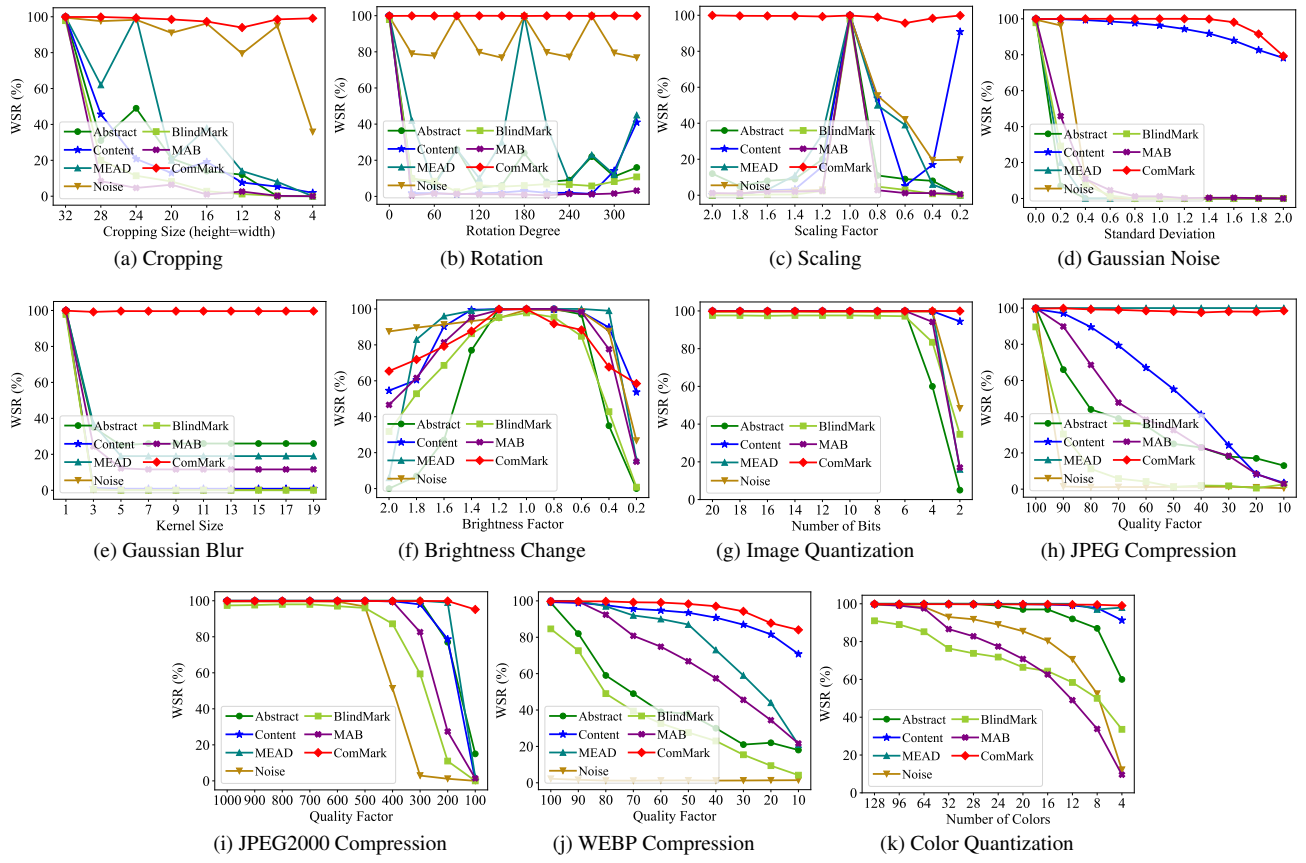


Figure 19. Comparison of robustness against watermark evasion attacks. (On CIFAR100)

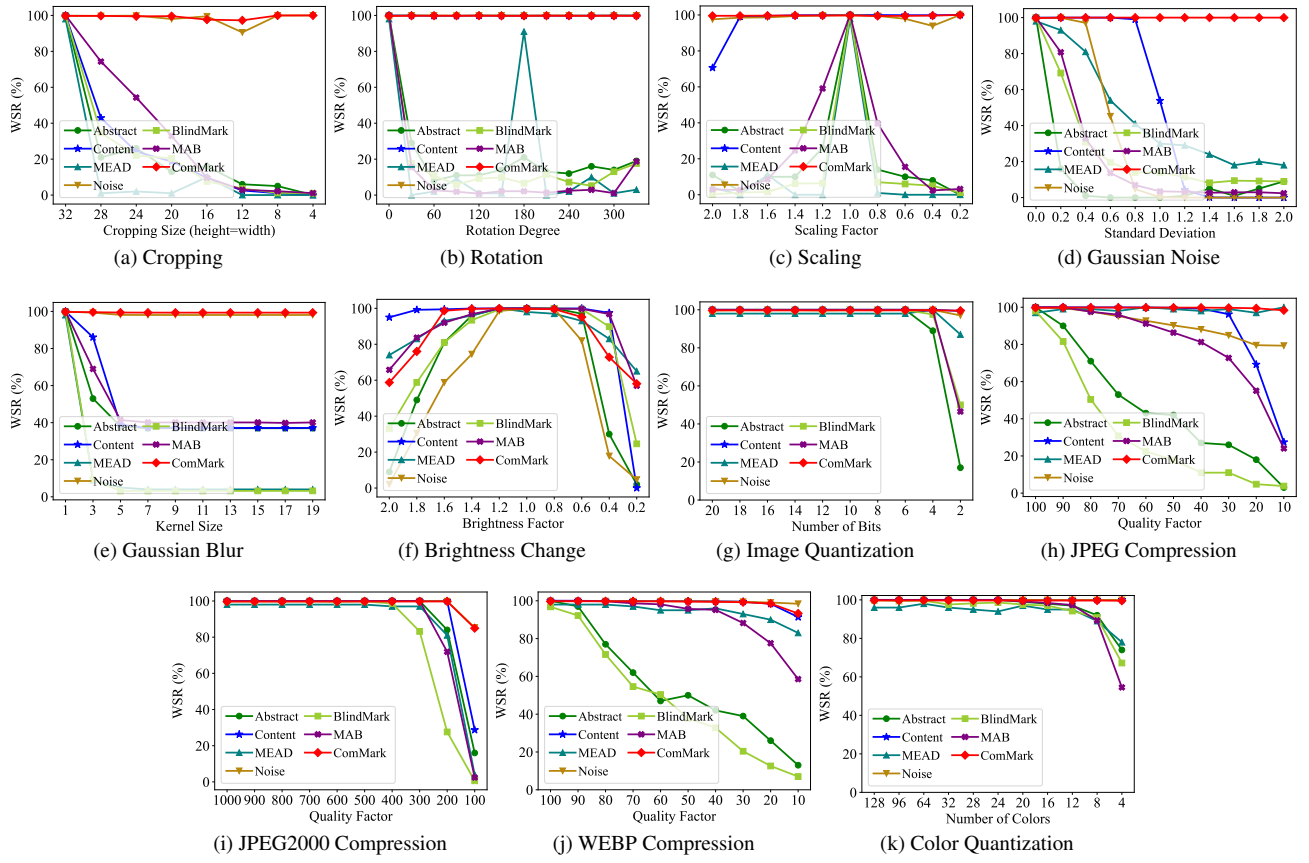


Figure 20. Comparison of robustness against watermark evasion attacks. (On VGGFace)